

**This is a self-archived version of an original article. This version may differ from the original in pagination and typographic details.**

**Author(s):** Lenngren, Nils; Edlund, Petra; Takala, Heikki; Stucki-Buchli, Brigitte; Rumfeldt, Jessica; Peshev, Ivan; Häkkänen, Heikki; Westenhoff, Sebastian; Ihalainen, Janne

**Title:** Coordination of the biliverdin D-ring in bacteriophytochromes

**Year:** 2018

**Version:** Accepted version (Final draft)

**Copyright:** © Royal Society of Chemistry, 2018

**Rights:** In Copyright

**Rights url:** <http://rightsstatements.org/page/InC/1.0/?language=en>

**Please cite the original version:**

Lenngren, N., Edlund, P., Takala, H., Stucki-Buchli, B., Rumfeldt, J., Peshev, I., Häkkänen, H., Westenhoff, S., & Ihalainen, J. (2018). Coordination of the biliverdin D-ring in bacteriophytochromes. *Physical Chemistry Chemical Physics*, 20(28), 18216-18225.  
<https://doi.org/10.1039/C8CP01696H>

# Coordination of the Biliverdin D-ring in Bacteriophytochromes

Nils Lenngren,<sup>a‡</sup> Petra Edlund,<sup>b‡</sup> Heikki Takala,<sup>a;c‡</sup> Brigitte Stucki-Buchli,<sup>a</sup> Jessica Rumfeldt,<sup>a</sup> Ivan Peshev,<sup>a</sup> Heikki Häkkinen,<sup>a</sup> Sebastian Westenhoff,<sup>\*b</sup> and Janne A. Ihalainen<sup>\*a</sup>

‡ Contributed equally

<sup>a</sup> Department of Biological and Environmental Sciences, Nanoscience Center, University of Jyväskylä, PO Box 35, FI-40014 University of Jyväskylä, Finland.

<sup>b</sup> Department of Chemistry and Molecular Biology, Biochemistry and Biophysics, University of Gothenburg, PO Box 462, SE-40530 Gothenburg, Sweden.

<sup>c</sup> University of Helsinki, Faculty of Medicine, Anatomy, PO Box 63, FI-00014 University of Helsinki, Finland.

\* corresponding authors: westenho@chem.gu.se, janne.ihalainen@jyu.fi

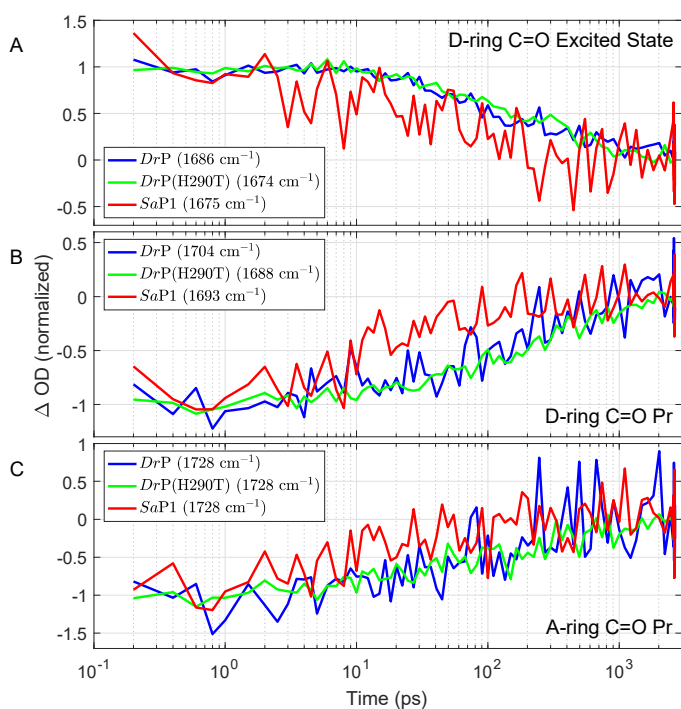


**Figure SI 1**, Normalized time traces of the IR signals of the carbonyl groups of the biliverdin at the excited state absorption (A), at the bleach of the D-ring (B), and at the bleach of the A-ring (C), of the *DrP*<sub>PSM</sub> (blue), *DrP*(H290T)<sub>PSM</sub> (green), and *SaP1*<sub>PSM</sub> (red) samples. The data shows that the excited state decay is faster in the case of *SaP1*<sub>PSM</sub> than the samples from *DrP*<sub>PSM</sub>, which show very similar decay profile irrespective to the H290T mutation.

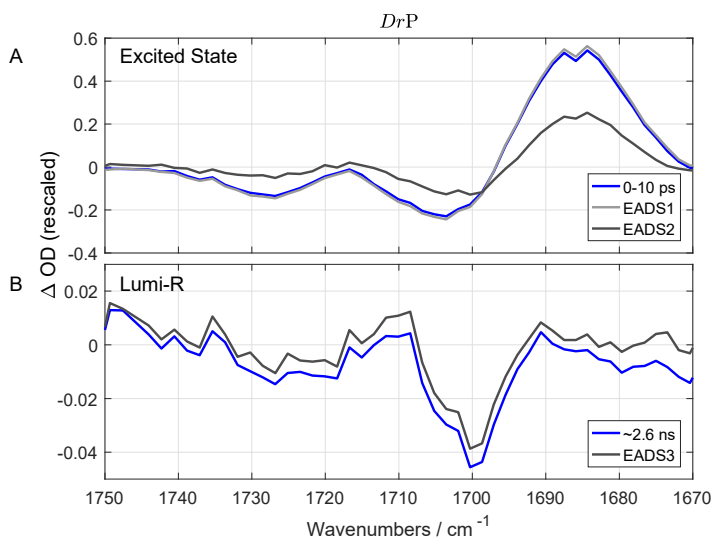


**Figure SI 2**, Comparison of the Evolution associated difference spectra and the raw spectral data at the early time points (A) and at the late time-points (B) of *DrP*<sub>PSM</sub>. The 2.6 ns spectral information is obtained by integrating signals from 30 different time-points within a distribution of 5 ps around the 2.6 ns. The detected spectrum at 1-10 ps overlays very well with the EADS and the spectral difference between EADS1 and EADS2 pinpoints the need of introduction of a second time-component to the analysis.

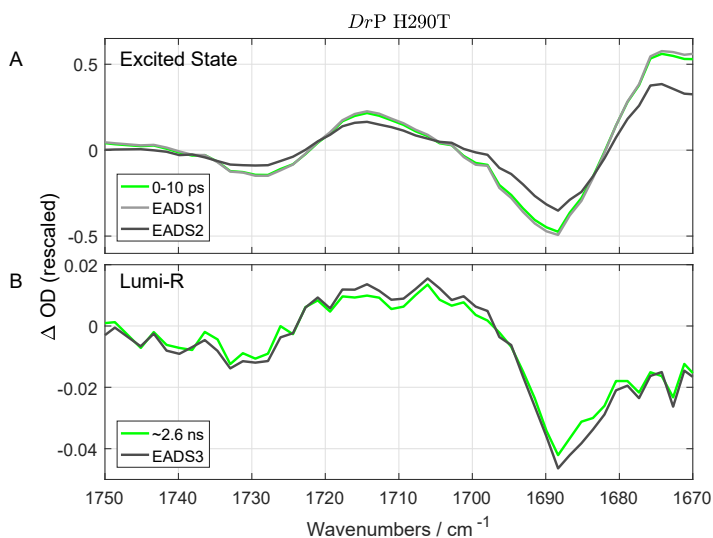


**Figure SI 3**, Comparison of the Evolution associated difference spectra and the raw spectral data at the early time points (A) and at the late time-points (B) of *DrP*(H290T)<sub>PSM</sub>. The 2.6 ns spectral information is obtained by integrating signals from 30 different time-points within a distribution of 5 ps around the 2.6 ns. The detected spectrum at 1-10 ps overlays very well with the EADS and the spectral difference between EADS1 and EADS2 pinpoints the need of introduction of a second time-component to the analysis.

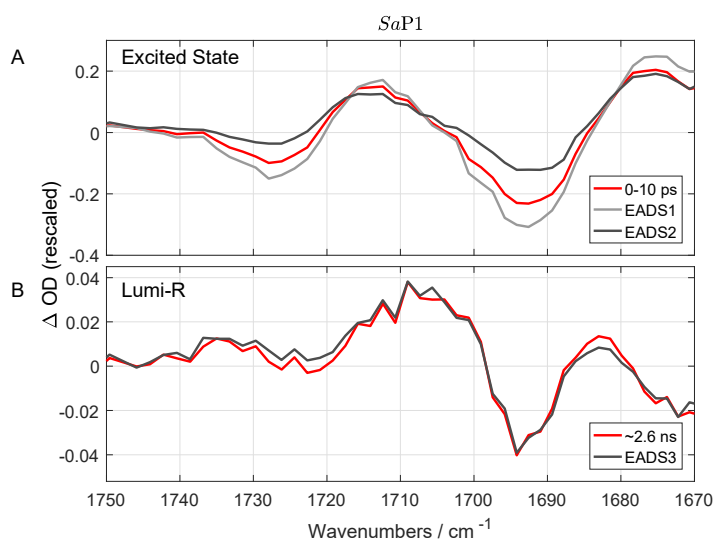


**Figure SI 4,** Comparison of the Evolution associated difference spectra (EADS) and the raw spectral data at the early time points (A) and at the late time-points (B) of *SaP1*<sub>PSM</sub>. The 2.6 ns spectral information is obtained by integrating signals from 30 different time-points within a distribution of 5 ps around the 2.6 ns. The spectral shape, detected at 1-10 ps , follows the spectral features of the EADS1. However, as the lifetime of the EADS1 is clearly shorter, the amplitude of the EADS1 is larger.